JOURNAL OF GUIDANCE, CONTROL, AND DYNAMICS
Vol. 15, No. 6, November-December 1992

Sensitivity of Space Station Alpha Joint Robust Controller to Structural Modal Parameter Variations

Renjith R. Kumar*
Analytical Mechanics Associates, Inc., Hampton, Virginia 23666
Paul A. Cooper†
NASA Langley Research Center, Hampton, Virginia 23665
and
Tae W. Lim‡
Lockheed Engineering and Sciences Company, Hampton, Virginia 23666

This paper describes the photovoltaic array sun tracking control system of Space Station Freedom. A synthesis procedure for determining optimized values of the design variables of the control system is developed by use of a constrained optimization technique. The synthesis is performed to provide a given level of stability margin, achieve the most responsive tracking performance, and meet other design requirements. Performance of the baseline design, which is synthesized using predicted structural characteristics, is discussed, and the sensitivity of the stability margin is examined for variations of the frequencies, mode shapes, and damping ratios of dominant structural modes. The design provides enough robustness to tolerate a sizeable error in the predicted modal parameters. The paper concludes with an investigation on the sensitivity of performance indicators as the modal parameters of the dominant modes vary, which would be useful in improving the control system performance if accurate modal data are provided through an on-orbit modal identification experiment.

Introduction

TO obtain electric power, Space Station Freedom (SSF), shown in Fig. 1, depends on photovoltaic (PV) solar arrays that track the sun during orbital daylight. The arrays are attached to deployable masts that are in turn attached through a rotary joint, called a solar beta rotary joint (beta joint), to the outboard portion of the transverse booms. The beta joint permits rotation of the arrays to compensate for the variation of the orbit plane with respect to the ecliptic plane. Rotary joints, called solar alpha rotary joints (SARJ, or alpha joints), regulate the relative rotational position of the outboard structure to the inboard structure. The attitude of the inboard structure is controlled by control moment gyros (CMGs) and reaction control system (RCS) jets. The alpha joints are used to orient the array surface normal vectors along the solar vector so that maximum solar energy falls on the arrays during the daylight portion of each orbit. The alpha joint control is designed to be a basic position tracking system with minor-loop velocity feedback to stabilize and provide damping to the rigid-body tracking motion. A proportional-integral (P-I) compensation is added in both the velocity and position loops to minimize steady-state tracking error.[1]

The allowable rigid-body control bandwidth of the alpha joint controller encompasses the resonant structural frequencies of the outboard boom and photovoltaic system so that the possibility for adverse interaction between the control system and the dynamic response of the structure exists. To reduce the possible detrimental effect of control/structure interaction, a low-pass filter is added to the velocity loop to attenuate the structural response signal. The proper placement of the corner frequency of the filter and selection of values for gain setting of the P-I compensation in the velocity and position loops are required to provide optimum performance. The proper selection of these design values depends on the accuracy of the predictions of the structural frequencies and modal response at sensor locations.

The space station is too large and flexible to support its own weight on Earth. Hence, the structural dynamic characteristics will have to be estimated from analytical models and component modal tests rather than from modal tests of the assembled structure. Further, the station is designed to support reconfigurations for more power, payload installations, and other activities that can change the dynamic characteristics of the station. Because of the considerable uncertainty involved in predicting the dynamic characteristics of the station initially and over its lifetime, the sun tracking control system must be designed with a high degree of stability robustness. This paper presents results from an investigation of the sensitivity of the control system stability margins to variations in modal parameters of dominant structural vibration modes. With this sensitivity established, the control system can be designed with a reasonable degree of robustness to ensure stable tracking for

Presented as Paper 91-2665 at the AIAA Guidance, Navigation, and Control Conference, New Orleans, LA, Aug. 12-14, 1991; received Oct. 9 1991; revision received March 4, 1992; accepted for publication March 27, 1992.

*Supervising Engineer. Member AIAA.
†Senior Engineer, Spacecraft Dynamics Branch, Mail Stop 246. Associate Fellow AIAA.
‡Senior Engineer, Langley Program Office, 144 Research Drive. Member AIAA.

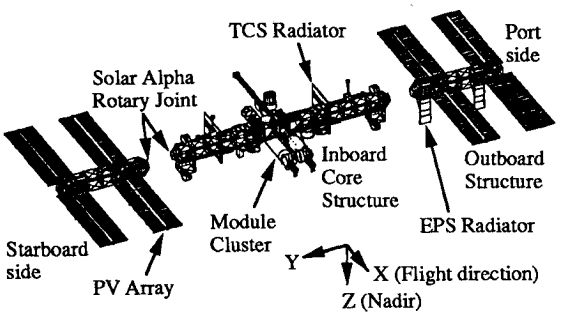

Fig. 1 Space Station Freedom assembly complete configuration.

a given range of variation in structural parameters that might occur due to configuration changes and errors in analytical estimation.

The paper describes the procedures used to attenuate the possible control/structure interaction and examine controller sensitivity to variations in structural modal parameters. First, the significant components of the space station related to the alpha joint control are described and the sun tracking control system is described. A baseline design is then determined using constrained optimization techniques to meet design requirements, provide a given level of stability margin, and obtain the most responsive tracking possible consistent with the assumed structural characteristics. Performance of the baseline design is discussed and the sensitivity of the stability margin is examined for variations of the natural frequencies, mode shape amplitudes, and modal damping ratios of the dominant structural modes. The paper concludes with an investigation of the sensitivity of performance index as the modal parameters of the dominant modes vary. The design variables are resynthesized for varying modal parameters to achieve the most responsive tracking performance while satisfying the design requirements.

Description of Space Station and Sun Tracking Function

Description of Space Station Structure

The space station structure can be broadly divided into an inboard core structure and an outboard articulating structure. As shown in Fig. 1, the inboard core structure is comprised of a module cluster, center truss, thermal control system (TCS) radiators, and various user payloads. The port and starboard truss, PV arrays, and electrical power system (EPS) radiators constitute the outboard articulating structure commonly referred to as the outboard structure. The attitude of the inboard core is maintained close to a local-vertical-local-horizontal (LVLH) orientation using active control devices such as the CMGs and/or RCS thrusters. The LVLH X axis is parallel to the flight direction, the LVLH Z axis is along the nadir, and the LVLH Y axis is orthogonal to the orbit plane. The power required for the space station is provided by the PV arrays as they track the sun. Because of the motion of the space station

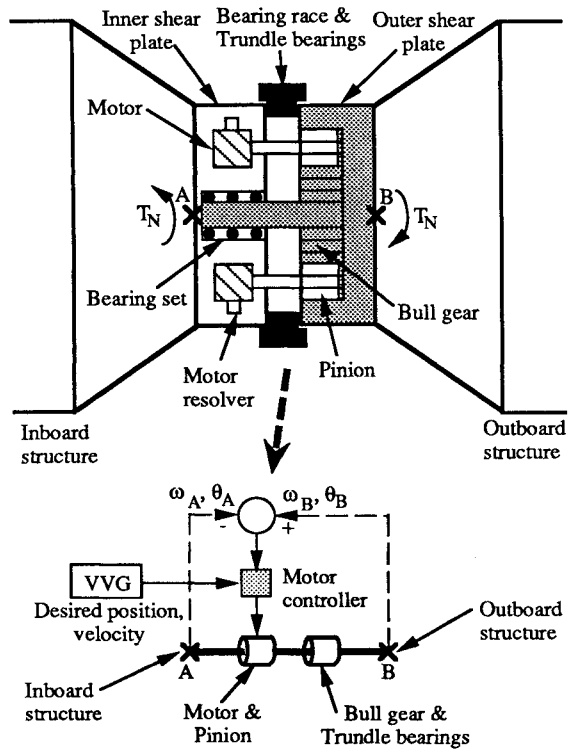

Fig. 2 Schematic of alpha joint drive train and control system.

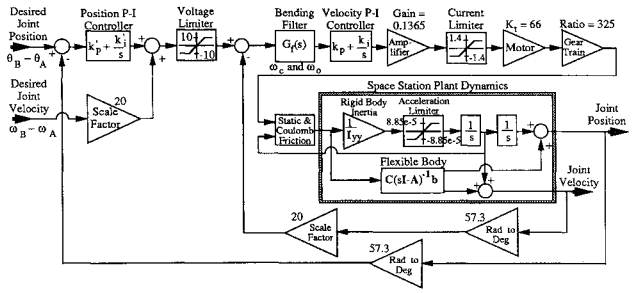

Fig. 3 Block diagram of solar alpha rotary joint control system.

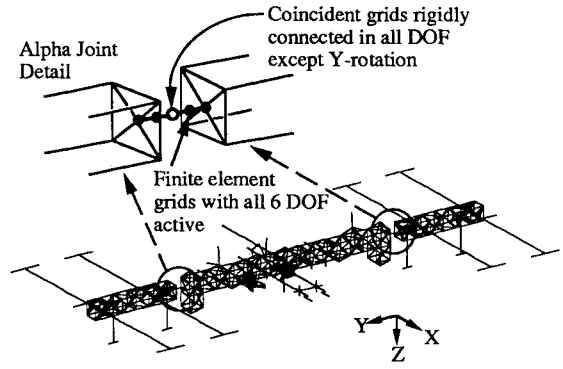

Fig. 4 Finite element model of Space Station Freedom.

along its orbit, core attitude fluctuations with respect to the LVLH orientation, and the variations of the orbit geometry with respect to the sun, the orientation of the PV arrays must be constantly adjusted with respect to the inboard core to track the sun. This function is performed by the alpha joints and the beta joints. The alpha joints provide a relative rotational motion between the inboard core structure and the outboard articulating structure. The beta joints perform the PV array orientation adjustment with respect to the articulating outboard port and starboard truss.

Assuming that the station is maintained at an LVLH attitude, the alpha joint rotation rate would be the orbital rate, completing a revolution every 90 min. The beta joint rotation is extremely slow over an orbit and closely follows the yearly variation of the orbit plane. Therefore, the beta joint drive and control is not addressed in this paper.

Physical Description of Alpha Joint

Each alpha joint consists of dual motors, dual resolvers, a motor controller, drive pinions, a bull gear, and trundle bearings, as depicted schematically in Fig. 2.[2] The motor provides the torque required to rotate the outboard structure. The amount of control torque provided by the motor is determined by the motor controller based on the measurements obtained by the joint resolver and the desired rotation data from the velocity vector generator (VVG) located on the inboard structure. The motor drive pinion to bull gear ratio has been carefully selected to minimize mechanical parts count and hence maximize reliability.[3] The bull gear is rigidly attached to the outboard structure through a shear plate. The large bull gear (~ 10 ft in diameter) is equipped with trundle bearings to accommodate large temperature gradients. The trundle bearings are the main source of friction. A set of high-power roll rings (not shown in Fig. 2) carries power across the joint as the joint rotates.[3]

Description of Alpha Joint Control System

The SARJ motor controller generates the required motor torque based on the difference between the desired and measured relative joint angular position and angular velocity at

Table 1 Summary of alpha joint controller design objective, variables, and constraints

Design objective	Maximize position and velocity loop bandwidth and minimize settling time
Design variables	Controller gains (k_p, k_p', k_i, and k_i') Compensation filter corner and zero frequencies (ω_c and ω_0)
Constraints	Rigid-body gain margins $\geq$ 6 dB Rigid-body phase margins $\geq$ 45 deg Apparent gain margins in structural resonant frequency range $\geq$ 20 dB Minimum rigid-body and controller damping ratio $\geq$ 0.5 Bandwidth between 0.01 and 1 Hz Steady-state pointing error $\leq$ 0.58 deg Jitter $\leq$ 0.01 deg/s

points A and B as shown in Fig. 2. Point A is fixed to the inboard structure, and point B is located on the outboard structure. The desired relative joint velocity command is determined by the VVG located on the inboard structure and is an input to the SARJ motor control system. As the SARJ position leads or lags the desired position (also provided by the VVG), the input to the velocity loop is increased or decreased to compensate for the position error. Hence, the reference input to the control system includes the desired relative angular velocity ($\omega_B - \omega_A$) and the desired relative angular position ($\theta_B - \theta_A$).

The detailed control system used in this paper is based on the design obtained from the SSF preliminary design review document.[4] A block diagram of the control system is shown in Fig. 3. The control system consists of an inner velocity servo loop that tracks the desired joint velocity and an outer position servo loop that increases or decreases the velocity command, depending on the position error. The velocity command is converted to a voltage command, and the maximum allowable SARJ velocity is maintained by a voltage limiter.

The inner servo loop includes a fourth-order Butterworth low-pass filter[5] with two additional zeros to roll off the high frequency structural modes. The two additional zeros are included to reduce the loss of rigid-body phase margin due to phase shift. The transfer function of the filter is

$$G_f(s) = \frac{\omega_c^4(s^2/\omega_0^2 + 1.4s/\omega_0 + 1)}{s^4 + 2.6\omega_c s^3 + 3.4\omega_c^2 s^2 + 2.6\omega_c^3 s + \omega_c^4} \quad (1)$$

where the corner frequency ω_c and the frequency of the zeros ω_0 are design variables.

While the inner velocity feedback loop increases system damping, it also increases steady-state tracking error. Integral control helps to reduce steady-state errors. Therefore, a P-I controller is used for the inner velocity loop and a similar P-I controller is used for the outer position loop. The position loop has a double integrator (one in the outer loop and the other in the inner loop) to track a ramp signal with zero steady-state error. The P-I controllers are also provided with integration limits to prevent the system from being overdriven.[4] This is required because of the acceleration limits imposed on the SARJ. Each P-I controller has two gain settings: k_p and k_i are the proportional and integral gains for the velocity loop, and k_p' and k_i' are the corresponding gains for the position loop. These are also included as design variables during the synthesis of the control system design.

The power amplifier shown in Fig. 3 is accompanied by a current limiter. A 66 in.-lbf/A motor torque constant and a gear ratio of 325 are assumed.[4] The output torque from the gear is subject to the large static and dynamic friction of the trundle bearings. The output torque must exceed the static friction of 3580 in.-lbf to initiate motion of the SARJ. Once the motion is initiated, a net torque, which exceeds the dynamic friction of 2870 in.-lbf, is applied to the structure at point B (actuator point) as shown in Fig. 2.

A finite element model of the space station structure is used to compute the natural frequencies and mode shapes. A flexible body state space model of the structure is formed from the modal data. This is combined with the rigid-body model of the outboard structure to characterize the dynamics of the space station structure. The rigid-body inertia of the outboard structure (either port or starboard side) about the Y axis (I_{YY}) is 1.75×10^7 lbf-in.-s^2. Details of the finite element model and modal description are given in the next section. The net torque T_N applied to the structure at actuator point B (Fig. 2) causes motion of the flexible structure. The T_N applied on the outboard structure causes a reaction torque on the core structure. This reaction torque has to be compensated by RCS jet and/or CMG torques to maintain the attitude of the core structure. This paper assumes that the reaction torque is compensated ideally and the rigid-body attitude of the core structure remains stationary. The joint position and velocity containing both rigid-body and elastic components are measured and fed back to close the control system loops.

Dynamic Characteristics of Space Station Freedom

A finite element model of SSF was used to investigate the influence of elastic response to the alpha joint control system performance. To provide a rotational degree of freedom (DOF) about the Y axis of the outboard structure, two coincident grids were placed at the center node of the alpha joint as indicated in Fig. 4. These grids are rigidly connected in the other five DOF. For the model used, there are 240 modes below 5 Hz, including the eight rigid-body modes.

Since the outboard structure is subject to a continuous rotational motion while the SARJ is actively controlled, the influ-

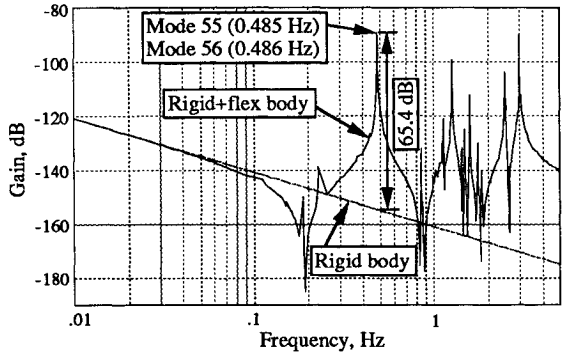

Fig. 5 Frequency response of rigid-body and rigid and flexible body plants (velocity response to control torque).

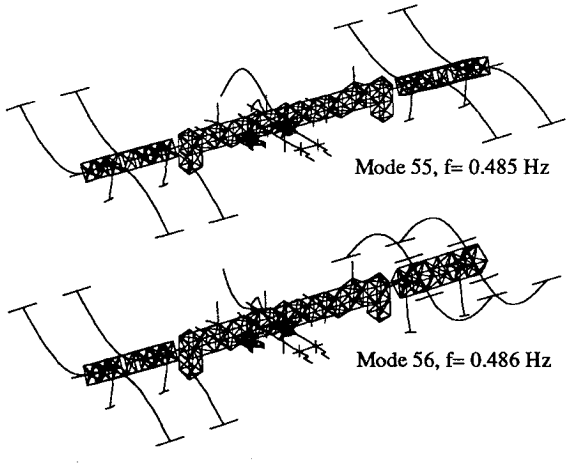

Fig. 6 Dominant modes for Space Station Freedom alpha joint control.

ence of the outboard structure orientation on the Space Station Freedom dynamic characteristics was investigated. The outboard structure was rotated 90 deg from the minimum drag PV orientation shown in Fig. 4 and the natural frequencies and mode shapes were calculated. The resulting maximum drag PV orientation SSF exhibits a natural frequency distribution almost identical to that of the minimum drag orientation. Also, the transfer function characteristics between the two points where the SARJ controller is applied (points A and B in Fig. 2) were almost identical. Thus, the dynamics of SSF with respect to the SARJ control is considered to be time invariant for this study. Moreover, because of the symmetry of the space station structure, the dynamic characteristics of the SARJ at the port and starboard sides are nearly identical. Thus, as a representative plant model, the port SARJ with a minimum drag PV array orientation is employed in this paper.

The equation of motion governing the flexible response at the port SARJ is represented by

$$\dot{x} = Ax + bu$$

$$y = Cx \tag{2}$$

where u is the control torque, and

$$x = \begin{Bmatrix} q \\ \dot{q} \end{Bmatrix}, \quad A = \begin{bmatrix} 0 & I \\ -\Omega^2 & -2Z\Omega \end{bmatrix}, \quad b = \begin{Bmatrix} 0 \\ \phi_B^T \end{Bmatrix}$$

$$y = \begin{Bmatrix} \theta_B - \theta_A \\ \omega_B - \omega_A \end{Bmatrix}, \quad C = \begin{bmatrix} \phi_B - \phi_A & 0 \\ 0 & \phi_B - \phi_A \end{bmatrix}$$

where q is the modal displacement vector, θ_A and θ_B are the angular displacements at points A and B, respectively; $\Omega = \text{diag}\{\omega_i\}$ and $Z = \text{diag}\{\zeta_i\}$, in which ω_i and ζ_i are the natural frequency and modal damping ratio of the ith mode, respectively; and ϕ_A and ϕ_B are the row vectors of the unity mass normalized mode shape matrix corresponding to the Y-rotational DOF at the points A and B, respectively. A modal damping ratio of 0.1% for all of the flexible modes is assumed as a baseline value for the design and simulation of the SARJ control system.

Synthesis Procedure of Control System Design Variables

Control System Requirements

The SARJ control system discussed earlier has six design variables with values that can be adjusted to optimize control system performance and satisfy prescribed requirements. The control system requirements can be classified as frequency-domain and time-domain requirements The frequency-domain requirements in both inner and outer loops are as follows: 1) Rigid-body open-loop gain margins (GMs) and phase margins (PMs) must be $\geq$ 6 dB and 45 deg, respectively, to ensure a stable rigid-body motion; 2) apparent gain margin (AGM), defined as the minimum distance of the open-loop gain from the 0-dB line in the frequency range encompassing the structural resonance frequencies, should be at least 20 dB to guarantee sufficient stability robustness to uncertainties in the predicted modal parameters; and 3) the closed-loop poles associated with the rigid body and controller should have a minimum damping ratio of 0.5. By constraining rigid body and controller closed-loop poles to a prescribed sector in the complex plane, this frequency-domain constraint ensures low overshoot during the transient response. The time-domain requirements[4] include small steady-state pointing errors and low jitter. The jitter is defined as the peak-to-peak variation of the position error in 1 s.

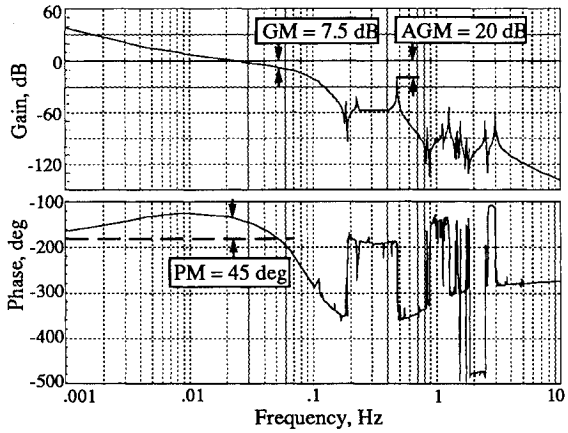

Fig. 7 Compensated Bode plot of port velocity open loop.

The preliminary design review document[4] requires that the inner and outer closed-loop bandwidths (BW_v and BW_p) be between 0.01 and 1 Hz. This requirement is treated in this paper as part of a performance index that is to be maximized. Bandwidth is a measure of the responsiveness of a control system (closely related to the rise time) and also represents a disturbance rejection threshold. Core attitude fluctuations and the maneuvers for feathering and debris collision avoidance may demand large attitude rate changes and thus motivate higher responsiveness of the control system. The other component of the performance index to be maximized is the magnitude of the real part of the dominant rigid-body and controller closed-loop pole σ. The dominant pole is defined here as the rigid-body and controller closed-loop pole (for both inner and outer loops) closest to the imaginary axis. This is equivalent to minimizing a settling time in a time-domain analysis. Table 1 summarizes the design objective, the control system frequency-domain and time-domain requirements, and the design variables.

Synthesis Procedure

The plant model includes the rigid-body inertia of the outboard structure about the alpha joint axis and the flexible modes of the entire structure. Figure 5 shows a frequency response function (FRF) of the rigid plant only compared with the FRF of the rigid body with all flexible modes of the finite element model up to a frequency of 5 Hz. The FRF shown is the magnitude ratio of the velocity response to net torque applied and is plotted using a decibel scale against the log of the frequency. A control system designed with only the rigid plant taken into account could become unstable if the dominant flexible modes are not well attenuated by the control system. The dominant flexible modes (or dominant modes) are the most influential modes among the flexible modes in determining the apparent gain margin. The flexible modes are most likely to be influential if their gain is high and their frequency is low. Figure 5 indicates that the dominant flexible modes occur at frequencies of 0.485 and 0.486 Hz. The corresponding mode shapes are shown in Fig. 6. These modes correspond to a rigid-body rotation of the outboard trusses coupled with symmetric and antisymmetric bending of the PV arrays while most parts of the inboard structure remain stationary. Other modes that might interfere with rigid-body controllers are at higher frequencies. Even though their gains might be higher than the modes selected as dominant, their influence would be further attenuated by a low-pass filter used to roll off the effects of the dominant modes and can hence be ignored during the control system design.

It is desirable that all of the flexible modes be removed from the plant during the synthesis of design variables to ease the computational load. The dominant flexible modes have a gain of $\sim$65.4 dB above the rigid-body gain as shown in Fig. 5.

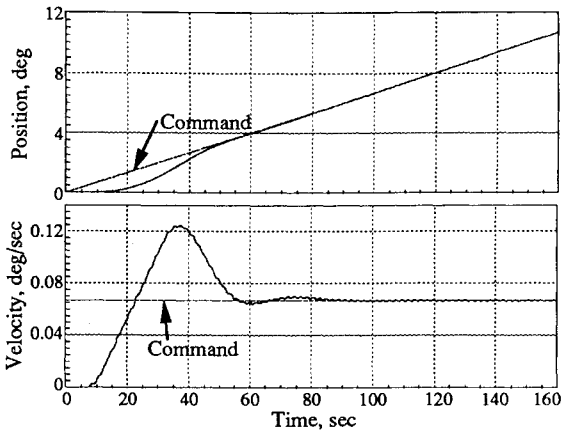

Fig. 8 Simulated position and velocity tracking response.

Hence, the 20-dB apparent gain margin constraint for the plant with the flexible modes is equivalent to a constraint of 85.4-dB apparent gain margin for the rigid-body plant at the frequency of 0.49 Hz. For the synthesis of design variables, the plant is considered as a rigid body with one of the constraints modified as described earlier. This consideration is used only for design purposes and is not for subsequent frequency response analyses or time response simulations.

To further simplify the synthesis procedure, the limiters in the control system are ignored. The friction block is replaced by a transfer function of unity, which is a conservative assumption for a robust design. The linearized plant and control system are transformed to the frequency domain, and the design synthesis is performed using a constrained optimization scheme.

Now the synthesis problem can be stated as follows: Find the optimum values for the six design variables (ω_c, ω_0, k_p, k_i, k_p', and k_i') that maximize the performance index

$$J = \mu_1 BW_v + \mu_2 BW_p + \mu_3 \sigma \tag{3}$$

while satisfying the following constraints:

1) velocity-loop rigid-body gain margin ≥ 6 dB;
2) position-loop rigid-body gain margin ≥ 6 dB;
3) velocity-loop rigid-body phase margin ≥ 45 deg;
4) position-loop rigid-body phase margin ≥ 45 deg;
5) velocity-loop rigid-body gain at the frequency of 0.49 Hz ≤ -85.4 dB; and
6) minimum rigid-body position and velocity closed-loop damping factor ≥ 0.5.

The scalars μ_1, μ_2, and μ_3 are weighting factors selected to give equal weights to each element of the performance index. Equal weights of unity are used for μ_1 and μ_2 since the velocity and position closed-loop bandwidths are of the same magnitude. The magnitude of σ is an order of magnitude less than the bandwidths and is expressed in radians per second. To give approximately equal importance to the settling time, $\mu_3 = 10$ is selected. The control torque is not incorporated in the synthesis problem either as a performance index or as a constraint. It is assumed that the available control torque will be sufficient to perform the maneuver required by the synthesized design.

The constrained optimization problem is solved using a nonlinear programming method available in MATRIXx software.[6] The software uses the Karmarkar's interior point algorithm. It was noticed that more than one local minimum existed for the optimization problem; thus, selection of the initial guess values for the six design variables was important for obtaining the "best" local minimum. However, one cannot be guaranteed that this best local minimum obtained is the global minimum.

The resulting optimized values of the design variables and the performance index are as follows: $\omega_c = 0.54$ rad/s, $\omega_0 = 3.83$ rad/s, $k_p = 0.73$, $k_i = 0.016$, $k_p' = 1.07$, $k_i' = 0.023$, $BW_v = 0.053$ Hz, $BW_p = 0.027$ Hz, and $\sigma = 0.026$. The design satisfies all of the prescribed design requirements. The steady-state time-domain requirements listed in Table 1, which were not enforced during the optimization, were checked for violation using the optimized design variables through time response simulation. The closed-loop poles of the velocity and position loops were inspected to ensure stability. The following section discusses the design results in detail.

Design Results

The bandwidths of the velocity and position loops are within the range specified in the space station program requirements. Design constraints are all met near or at the boundary of the constraints. The compensated Bode plot of the velocity loop on the port side of the station is shown in Fig. 7. All of the flexible modes below 5 Hz were incorporated into the simulation. An apparent gain margin of 20 dB and rigid-body gain and phase margins of 7.5 dB and 45 deg, respectively, are obtained as indicated in the figure.

The time response of the control system is simulated for a step velocity command of 4 deg/min and a ramp position command with a slope of 4 deg/min. Figures 8 and 9 show the results of the simulation using all of the flexible modes below 5 Hz. The position command input and the resulting response are compared in Fig. 8. No motion occurs until the static friction is overcome. Then, after a brief initial transient period, the tracking is performed accurately. The velocity response to the command is also shown in Fig. 8. The higher frequency component of the response corresponds to the flexible response of the structure at the dominant mode frequency. The flexible response is quite small and should cause no structural load problems. The steady-state pointing error, which should be < 0.58 deg, is met within 40 s, and the steady-state jitter requirement is met in < 1 min.

Figure 9 illustrates the torque generated by the motor and gear train to perform the alpha joint pointing and the net torque applied to the station after overcoming the friction. No net torque is applied to the station until the torque overcomes the static friction. Once the motion of the alpha joint is initiated, the dynamic friction becomes effective and the magnitude of steady-state motor/gear torque is just enough to overcome the dynamic friction. As a result, the core structure of the station does not experience a net torque applied from the joint motor and gear train after the initial transient period of 100 s. The maximum torque available is ~30,000 in.-lbf. The peak motor torque required is well within the torque limit. Therefore, the assumption that the motor is capable of producing the level of torque required by the synthesized design is verified.

Sensitivity of Stability Robustness and Performance to Structural Parameter Variations

The flexible plant model used in the synthesis of design variables is characterized by natural frequencies, mode shapes, and modal damping ratios. The baseline design variables pre-

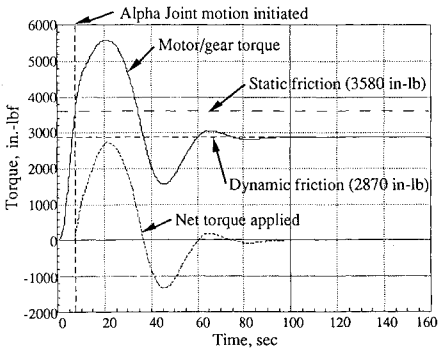

Fig. 9 Simulated motor/gear torque and net torque applied.

sented in the preceding section were obtained using "nominal" values of the modal parameters. These nominal modal parameters are analytical estimates and may be inaccurate. To address the effect of variation of the modal parameters on the control system performance, two types of sensitivity analyses are performed in this paper. The first study examines the change in the apparent gain margin (stability robustness measure) as the modal parameters vary while the baseline values of the design variables are maintained. In the second study the values of the design variables are resynthesized for the flexible plant with modified modal parameters while the same design constraints are enforced as those used for the baseline design. The resulting variation of the performance index is investigated. For a set of fixed values of the design variables, the performance index is independent of the changes in structural modal parameters because the performance index is composed of the velocity and position loop bandwidths and the dominant rigid-body closed-loop pole. Thus, performance robustness due to structural parameter variation is not discussed in this paper.

Sensitivity of Stability Robustness

While the baseline values of the design variables are kept unchanged, the effect of modal parameter changes on the stability margin is examined. The gain and phase margins of the position and velocity loops and the locations of the rigid-body plant and controller poles remain unchanged since the values

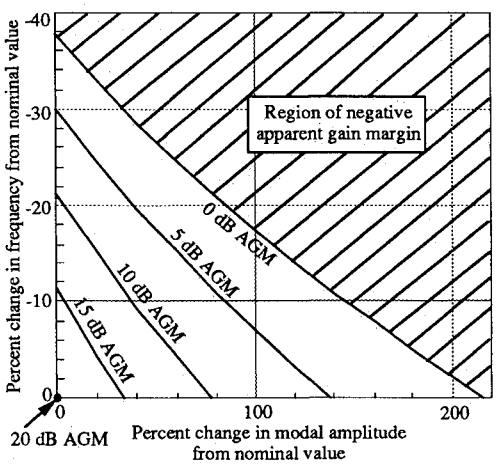

Fig. 10 Sensitivity of velocity-loop apparent gain margin to variations in frequency and modal amplitude of dominant elastic mode (modal damping = 0. 1%).

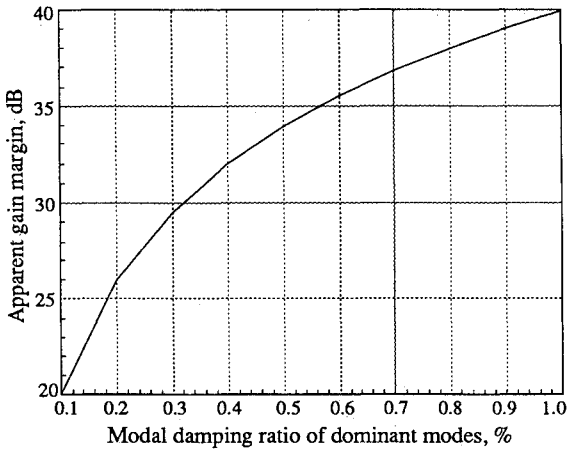

Fig. 11 Sensitivity of velocity-loop apparent gain margin to variations in modal damping ratio of dominant modes.

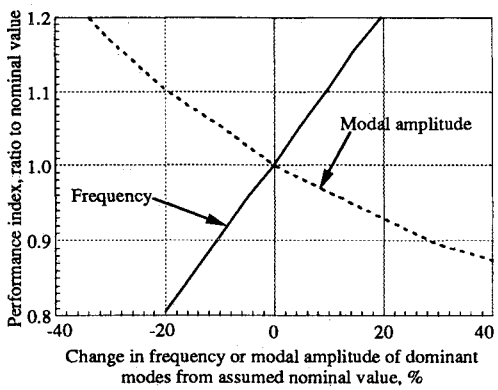

Fig. 12 Sensitivity of performance index to variations in frequency or modal amplitude from assumed nominal values.

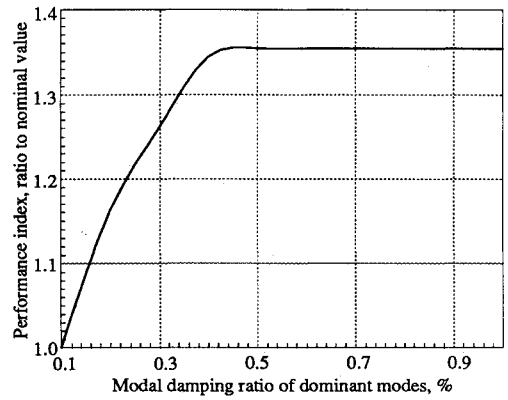

Fig. 13 Sensitivity of performance index to variations in modal damping ratio of dominant modes.

of the design variables and rigid-body plant are fixed for this study. Only the apparent gain margin is influenced by the variation of the modal parameters. The baseline design parameters obtained for the nominal flexible plant provide 20-dB velocity-loop apparent gain margin at the frequencies of dominant modes. The position loop always has a larger apparent gain margin. Therefore, this study examines only the change in the velocity-loop apparent gain margin as the modal parameters of the dominant modes vary.

Figure 10 shows the sensitivity of stability margin to a variation in dominant mode frequencies and modal amplitudes while the modal damping ratio is held constant at 0.1%. Lines of constant apparent gain margins are shown in the figure. Changes in modal frequencies affect only the system A matrix. The modal amplitude is varied by positive scalar multiplications of the mass normalized mode shapes at the sensor and actuator locations simultaneously. These affect the system b vector and C matrix. All modal parameter variations are represented in percentages.

As the dominant mode frequencies decrease, the resonant peaks of the two dominant modes move closer to the corner frequency of the bending filter ω_c. Hence, the amount of rolloff at the dominant mode frequencies decreases, resulting in a smaller apparent gain margin. This is indicated along the ordinate of Fig. 10. When the dominant mode frequencies are decreased by $\sim 38\%$ while the modal amplitude is held constant, the apparent gain margin diminishes to zero, and if the phase at this frequency is at -180 deg, the system becomes unstable. The origin corresponds to the nominal plant. It should also be noted that the robustness would be improved if the dominant mode frequencies are increased (not shown in Fig. 10). The reduction in robustness for a given frequency change is seen along the abscissa of Fig. 10 as the modal amplitude increases. The increase in modal amplitude corre-

sponds to the increase in height of the resonant peaks and hence reduces the apparent gain margin. A change of approximately +210% in the modal amplitude of the dominant modes is required to nullify the apparent gain margin. A reduction in modal amplitude increases the apparent gain margin (not shown in Fig. 10).

Points interior to the axes correspond to combined errors in both modal frequencies and modal amplitudes. Regions of negative stability margins are also shown in Fig. 10. Space station structural parameters predicted analytically may contain appreciable errors.[7] The inability of ground testing for model verification and the synthesis error of component modal characteristics are the major source of the errors. Thus, to compensate for the errors, the control system design should be robust to large variations in modal parameters. Figure 10 indicates that, for a nominal design using a 20-dB apparent gain margin, the control system can tolerate a wide range of modal parameter variations.

Figure 11 depicts the sensitivity of stability robustness to a variation in modal damping ratio while the dominant mode frequencies and modal amplitudes are held constant. The nominal plant has a conservative low damping of 0.1%. As the modal damping ratio increases, the resonant peak of the dominant modes decrease (the resonant peak is approximately proportional to $1/2\zeta$). Thus, the apparent gain margin increases. As the modal damping ratio decreases, the apparent gain margin decreases. However, this is not discussed due to the already conservative nominal value of modal damping ratio chosen.

Sensitivity of Control System Performance

In this study the control system design variables are resynthesized as the modal parameters of the dominant modes vary. The constraints, as listed in Table 1, are enforced and the values of the design variables are recomputed for each change in the value of a modal parameter to provide the most responsive tracking performance. The variation of the performance index is examined as the frequencies, modal amplitudes, and modal damping ratios change.

Figure 12 (solid line) shows the variation of the performance index as the frequencies of the dominant modes change. The modal amplitudes and damping ratios are held at their nominal values. The ordinate is the ratio of the performance index J to its nominal value. The performance index consistently improves as the dominant mode frequencies increase and vice versa. As the dominant mode frequencies increase, the passband of the Butterworth filter can be extended. This results in an increase in the performance index. The design variables are resynthesized at the interval of 5% change in nominal frequency. For instance, the baseline design variables are used as an initial guess for the synthesis with 5% frequency change. Figure 12 (broken line) illustrates the variation of the performance index as the modal amplitude of the dominant modes changes. The frequencies and modal damping ratios are fixed at their nominal values. The performance index consistently decreases with increasing modal amplitude. As the resonant peaks of the dominant modes increase, the apparent gain margin constraint is violated. To meet the constraint, the corner frequency of the filter decreases while ensuring that the other constraints are not violated. Thus, the performance index decreases. The design variables are resynthesized at intervals of 10% change in nominal modal amplitude using the previous optimized design as a starting guess for design variables.

The variation in the performance index with respect to the changes in modal damping ratios is shown in Fig. 13. As the modal damping ratio increases, the resonant peaks of the dominant flexible modes reduce and the apparent gain margin constraint becomes less critical. The passband of the low-pass filter may be extended, increasing the bandwidth until the apparent gain margin constraints or the other constraints become active. Hence, the performance indicators should increase or at worst remain constant. Figure 13 indicates that the performance increases until the modal damping ratio is raised to approximately ~0.4%. At this value, the apparent gain margin constraint is no longer active and the performance index remains constant for additional increase in damping. Thus, attempts to increase the modal damping ratio would be beneficial in increasing control system performance only up to a certain level. The magnitude of modal damping ratio at which this performance saturation occurs will depend on the constraints imposed.

The time-domain analysis for each set of optimized values of the design variables should be performed so that it can be determined whether the steady-state pointing and jitter requirements are satisfied. The time-domain response will depend on the values of the design variables but will damp out since the closed-loop rigid-body pole constraint ensures a minimum damping ratio of 0.5. The steady-state tracking errors could be met by adjusting the integrator limits in the controllers.

Conclusions

A baseline design of the Space Station Freedom solar alpha rotary joint control system is described in this paper. A synthesis procedure for determining optimized values of the design variables of the control system was developed using constrained optimization techniques to meet design requirements, provide a given level of stability robustness, and obtain the most responsive tracking capable consistent with the assumed structural characteristics. Performance of the baseline design was discussed and the sensitivity of the stability margin was examined for variations in the natural frequencies, mode shapes, and damping ratios of dominant structural modes. The design provided enough robustness to tolerate a sizeable error of up to 40% in the predicted resonant frequency of the dominant modes and to tolerate an error in the predicted modal amplitude of up to 200%. The station will not be tested as a complete system before being placed in orbit, and modal frequencies will have to be predicted using information from component tests and unvalidated analytical models. Hence, the high levels of stability margin suggested in this study for the nominal design seem appropriate. The paper concludes with an investigation on the sensitivity of performance indicators as the modal parameters of the dominant modes vary. The design variables are resynthesized for varying modal parameters to achieve the most responsive tracking performance while satisfying the design requirements. This procedure of reoptimizing design parameters would be useful in improving the control system performance if accurate modal data are provided through an on-orbit modal identification experiment.

References

[1]Laskin, R. A, Estus, J. M., Lin, Y. H., Spanos, J. T., and Scatter, C. M., "NASA Office of Space Science and Applications Study on Space Station Attached Payload Pointing," *Proceedings of AIAA Guidance, Navigation, and Control Conference* (Minneapolis, MN), AIAA, Washington DC, 1988, pp. 430–443 (AIAA Paper 88-4105).

[2]Merritt, L. V., "Rotary Joint Servo Loops: General Description with Performance Models," Lockheed Missiles & Space Company, Rough Draft of EM-2-ME-62, Space Station Work Package 2, Sunnyvale, CA, March 1990.

[3]Merritt, L. V., "The Space Station Rotary Joint Motor Controller," *Motion Journal,* Jan.–Feb. 1990, pp. 14–22.

[4]Bone, J., and Nuttall, N., "Performance Assessment of the Solar Alpha Rotary Joint Control System with a Flexible Dynamic Load Model," EM-2-ME-014, PDR document MDC H6506, Space Station Work Package 2, June 1990.

[5]Lam, H. Y-F., *Analog and Digital Filters: Design and Realization,* Prentice-Hall, Englewood Cliffs, NJ, 1979, p. 301.

[6]*MATRIXx Optimization Module Manual,* 2nd ed., Integrated Systems, Inc., Santa Clara, CA, Oct. 1989.

[7]Hanks, B. R., "Dynamic Challenges for 21st-Century Spacecraft," Keynote Address, 21st Shock and Vibration Symposium, Pasadena CA, Oct. 1990.